Published for SISSA by Springer

Received: *January 23, 2017*
Revised: *March 27, 2017*
Accepted: *April 18, 2017*
Published: *April 28, 2017*

# Augury of darkness: the low-mass dark $Z'$ portal

**Alexandre Alves,**[a] **Giorgio Arcadi,**[b] **Yann Mambrini,**[c] **Stefano Profumo**[d,e] **and Farinaldo S. Queiroz**[b]

[a] *Departamento de Física, Universidade Federal de São Paulo, Diadema-SP, 09972-270, Brasil*

[b] *Max-Planck-Institut fur Kernphysik, Saupfercheckweg 1, 69117 Heidelberg, Germany*

[c] *Laboratoire de Physique Théorique, CNRS — UMR 8627, Université de Paris-Saclay 11, F-91405 Orsay Cedex, France*

[d] *Department of Physics, University of California, Santa Cruz, 1156 High St, Santa Cruz, CA 95060, U.S.A.*

[e] *Santa Cruz Institute for Particle Physics, Santa Cruz, 1156 High St, Santa Cruz, CA 95060, U.S.A.*

*E-mail:* aalves@unifesp.br, arcadi@mpi-hd.mpg.de, yann.mambrini@th.u-psud.fr, profumo@ucsc.edu, queiroz@mpi-hd.mpg.de

Abstract: Dirac fermion dark matter models with heavy $Z'$ mediators are subject to stringent constraints from spin-independent direct searches and from LHC bounds, cornering them to live near the $Z'$ resonance. Such constraints can be relaxed, however, by turning off the vector coupling to Standard Model fermions, thus weakening direct detection bounds, or by resorting to light $Z'$ masses, below the Z pole, to escape heavy resonance searches at the LHC. In this work we investigate both cases, as well as the applicability of our findings to Majorana dark matter. We derive collider bounds for light $Z'$ gauge bosons using the $CL_S$ method, spin-dependent scattering limits, as well as the spin-independent scattering rate arising from the evolution of couplings between the energy scale of the mediator mass and the nuclear energy scale, and indirect detection limits. We show that such scenarios are still rather constrained by data, and that near resonance they could accommodate the gamma-ray GeV excess in the Galactic center.

Keywords: Cosmology of Theories beyond the SM, Beyond Standard Model

ArXiv ePrint: 1612.07282



doi:10.1007/JHEP04(2017)164

JHEP04(2017)164

## Contents



JHEP04(2017)164

## 1 Introduction

Non-baryonic dark matter (DM) accounts for about 27% of the energy budget of the universe [1]. Its particle nature is one of the most pressing puzzles at the interface of particle physics and cosmology. Several dark matter candidates have been extensively discussed and reviewed in the literature (see e.g. [2, 3]); among those, Weakly Interacting Massive Particles (WIMPs) stand out for arising in several compelling particle physics models, such as supersymmetry, for naturally accounting for the DM abundance in the universe through the thermal freeze-out paradigm, and for potentially being testable with current and future experimental probes (see e.g. [4–6]).

The key strategies for WIMP searches are direct, indirect, and collider searches. The former consist of measuring nuclear scattering events with recoil energies on the order of the keV in underground laboratories [7–10]. WIMP signals in a direct detection experiment are directly proportional to the local dark matter density, thus the observation of a signal can be strongly tied to the presence of WIMP scattering.

Indirect detection attempts to detect the stable Standard Model particle products of dark matter annihilation, such as gamma-rays, cosmic-rays, or radiation at lower frequency in the electromagnetic spectrum [11–15]. The signal observed is proportional to the integrated line-of-sight dark matter density squared in the region of interest.

Finally, collider searches hinge on the fact that high-energy proton-proton collisions at the LHC can generate dark matter particles in association with other exotic particles. The associated signature would consist of missing energy in, for instance, monojet or dijet searches. Whilst not capable to unveil the astrophysical connection of the particles produced, collider studies can provide a complementary and sometimes more effective way to constrain dark matter models [16], especially with light dark matter particles.

The efficacy of each detection strategy at probing WIMPs is rather model-dependent; however, and rather interestingly, for the model we focus on this paper, there is a remarkable degree of complementarity across direct, indirect, and collider searches.

The observation of WIMP events at any of the detection strategies would be paramount to understand the laws of nature at fundamental scales, since WIMPs are expected to be embedded in UV complete models such as the minimal superymmetric standard models or minimal left-right model [17–20]. In other words, the discovery of WIMPs is tightly related to uncovering hints about underlying physics beyond the Standard Model.

In order to map the interactions between WIMPs and standard model particles which are allowed by data, simplified models have become powerful tools. In particular, simplified models which make use of vector mediators [21].

Models with a $Z'$ neutral gauge boson portal between dark and ordinary matter have attracted significant attention for a variety of reasons: they for instance represent "simplified model" version of several compelling particle models, and are constrained by data in a rather stringent way, albeit the couplings of the new boson to dark and ordinary matter are largely model-dependent [22–32].

Assuming the dark matter particle to be a Dirac fermion, many analysis have been done in the context of heavy mediators ($M_{Z'} > 1\,\text{TeV}$) [33–62]. The key results are that these models are plagued with restrictive spin-independent direct detection limits as well as LHC bounds on the $Z'$ mass from heavy resonance searches, limiting the allowed parameter space to the $Z'$ resonance, i.e. when the mass of the dark matter is close to half the mass of the $Z'$.

In this work, we investigate an alternative scenario by turning off the vector coupling to Standard Model fermions as proposed in [42] to weaken direct detection bounds, and by focusing on relatively light $Z'$ masses, ($M_{Z'} < 500\,\text{GeV}$) , to circumvent the usual heavy-resonance searches at the LHC.[1]

The present analysis markedly differs from previous analysis for a variety of reasons:

(i) We focus on a very specific class of $Z'$ models, namely those where the $Z'$ possesses purely axial-vector couplings with SM fermions, and we perform a detailed dark matter phenomenology study;

(ii) We show that the $Z'$ mass can be as low as 15 GeV, where the heavy resonance searches at the LHC searches are not applicable. We explicitly compute the collider limits in that region, with no rescaling, using the $CL_S$ method employing dimuon data from the LHC;

[1]See also ref. [63] for an study on light $Z'$ bosons, focused on mono $Z'$ signatures at the LHC.



JHEP04(2017)164

(iii) We discuss the possibility of accommodating the gamma-ray excess observed in the Galactic center in the context of this class of models.

The paper is structured as follows. We introduce the model under consideration in section 2. Section 3 is devoted to a detailed study of the invisible $Z'$ searches at LHC, whereas direct detection constraints are analyzed in section 4. After a discussion on the Galactic center excess in section 6, we conclude.

## 2 Model

We investigate here a $\mathrm{U}(1)_X$ extension of the Standard Model expected to be less constrained by collider, direct and indirect detection searches. The model is based on the gauge group $\mathrm{SU}(3)_c \otimes \mathrm{SU}(2)_L \otimes \mathrm{U}(1)_Y \otimes \mathrm{U}(1)_X$. Augmenting the SM by a new Abelian symmetry implies the existence of a new gauge boson $Z'$, which can gain mass in different ways. To preserve gauge invariance such gauge boson will couple to SM fermion through the covariant derivatives $\bar{f}_L \gamma_\mu D^\mu f_L$ and $\bar{f}_R \gamma_\mu D^\mu f_R$, where $D^\mu = \partial^\mu - i\, g_f\, q_f Z'^\mu$, which lead to,

$$\mathcal{L} \supset i\bar{f}\gamma_\mu \left[\partial_\mu - i g_f \frac{q_{f\,L} + q_{f\,R}}{2} - i g_f \frac{q_{fR} - q_{fL}}{2}\gamma^5\right] f\, Z'^\mu \tag{2.1}$$

If $q_{fL} = q_{fR}$, i.e. the left and right-handed SM fermions transform in the same way under $\mathrm{U}(1)_X$ (vector-like fermions), the $Z'$ will have only vectorial couplings with SM fermions, corresponding to a dark photon. Conversely, if $q_{fL} = -q_{fR}$, only axial-vector current are non-vanishing. The latter is the scenario we are interested in. The addition of a Dirac fermion dark matter field is trivial and follows the same logic. Focusing on the latter the final Lagrangian reads

$$\mathcal{L} \supset \left[\bar{\chi}\gamma^\mu(g_{\chi v} + g_{\chi a}\gamma^5)\chi + g_f \bar{f}\gamma^\mu\gamma^5 f\right] Z'_\mu, \tag{2.2}$$

where $\chi$ is the dark matter candidate We remark that in order to write a Lagrangian of the form eq. (2.2) it is necessary to assume that SM fermions be charged under the $\mathrm{U}(1)_X$ symmetry. One should also notice that the model is clearly anomalous: due to the chirality of the SM fermions, the triangle anomalies $\mathrm{U}(1)_X^3$ do not cancel. Anomaly cancellation generically requires the existence of new fields. The new fields can, however, be vector-like under the SM gauge group, while being chiral under the new Abelian symmetry. With appropriate charge assignments one can construct an anomaly-free model where the $Z'$ has only axial-vector coupling to fermions. In ref. [64], the authors have put some effort in coming up with UV complete models where the eq. (2.2) is realized. We will thus assume that the exotic fermions needed to cancel the anomalies are sufficiently heavy so as not to spoil the dark matter phenomenology.[2] We emphasize that this assumption is crucial to the validity of our results, especially because we will be focusing on $Z'$ masses below 1 TeV.

All the numerical computations will be carried under the assumption $g_{\chi v} = g_{\chi a} = g_\chi$. Keeping them in the same order is arguably a natural choice. Mild departures from this

[2]This is not always possible, as argued in [64], since the exotic fermions may contribute to the renormalization group equation and affect the running of the couplings.



JHEP04(2017)164

assumption will change neither the relic density nor the annihilation cross section today since they are both dominated by the vectorial term. As for WIMP-nucleon scattering rates, the impact is also mild. However, had we set $g_{\chi v}$ to zero, we would have been discussing a Majorana fermion, where the annihilation cross section is helicity suppressed, and the WIMP-nucleon scattering is purely spin-dependent. An overall minus sign between the couplings will induce no change to our results. Furthermore, this choice conveniently reduces the number of free parameters of the simplified model. That said, as long as one does not dramatically deviates from $g_{\chi v} \sim g_{\chi a}$, our conclusions will readily apply.

## 3 Collider constraints on light $Z'$ models

Searches for high- and low-mass dilepton resonances at the LHC have been an excellent probe of models containing new neutral vector bosons [65, 66]. In the case where the new vector boson mediates the interaction between the SM and the dark sector, constraints from dijets and monojet searches for the $Z'$ are complementary in the *mass versus coupling* plane [36]. These are the most stringent constraints for leptophobic dark $Z'$ models. When couplings to leptons are sizable, though, dileptons searches have the potential to exclude larger portions of the models' parameter space [67–69] compared do dijets. This can be understood in view of the relative size of the production cross section for dijets and dileptons and their correspondent irreducible backgrounds: first, both production mechanisms are electroweak processes; second the dominant backgrounds for dijets and dileptons are the QCD jet pair production and the Drell-Yan processes, respectively. For universal fermion couplings as those assumed in this work, the relative number of flavors and color multiplicity leads to the relation (at LO) $\sigma(pp \to Z' \to jj)/\sigma(pp \to Z' \to \ell^+\ell^-) = 15$, where $\ell$ denotes electrons or muons. On the other hand, at LO, for the dominant backgrounds we have $\sigma(pp \to Z \to \ell^+\ell^-)/\sigma(pp \to jj) \sim \mathcal{O}(10^{-4})$ at the 13 TeV LHC [70], and a similar ratio should be expected at 7 and 8 TeV center-of-mass energies.

### 3.1 Signal simulation and branching ratios

In order to evaluate the constraints from the 7 TeV LHC data [65] below the $Z$ pole, and above it with 8 TeV data [66], we implemented the axial $Z'$ model in `FeynRules` [71] to simulate our signal events. We also obtained the partial widths for the $Z'$ decays to leptons, jets, dark matter pairs and top pairs. The branching ratios and cross sections depend on four basic parameters: $\{M_{Z'}, M_\chi, g_\chi, g_f\}$, the mass of the $Z'$, the dark matter mass, the $Z'$ coupling to $\chi$, and the (axial) $Z'$ coupling to the SM fermions, respectively.

In figure 1 we show the $Z'$ branching ratios as function of its mass for some benchmark points. In the upper left panel we fixed $M_\chi = 100\,\text{GeV}$ and $g_\chi = g_f = 0.1$. We see that decays to jets dominate, followed by invisible decays, from light to heavy $Z'$ masses, while the branching ratio to leptons (electrons or muons) is of order 3%. We also observe thresholds when the vector boson is heavy enough to decay to $\chi$ and top pairs. The picture is essentially the same as either $\chi$ gets heavier or the couplings are changed but kept equal to each other, as shown at the upper right panel and the lower left panel. However, the branching ratio to dark matter reaches almost 90% when $g_\chi \gg g_f$. In this regime it is



JHEP04(2017)164

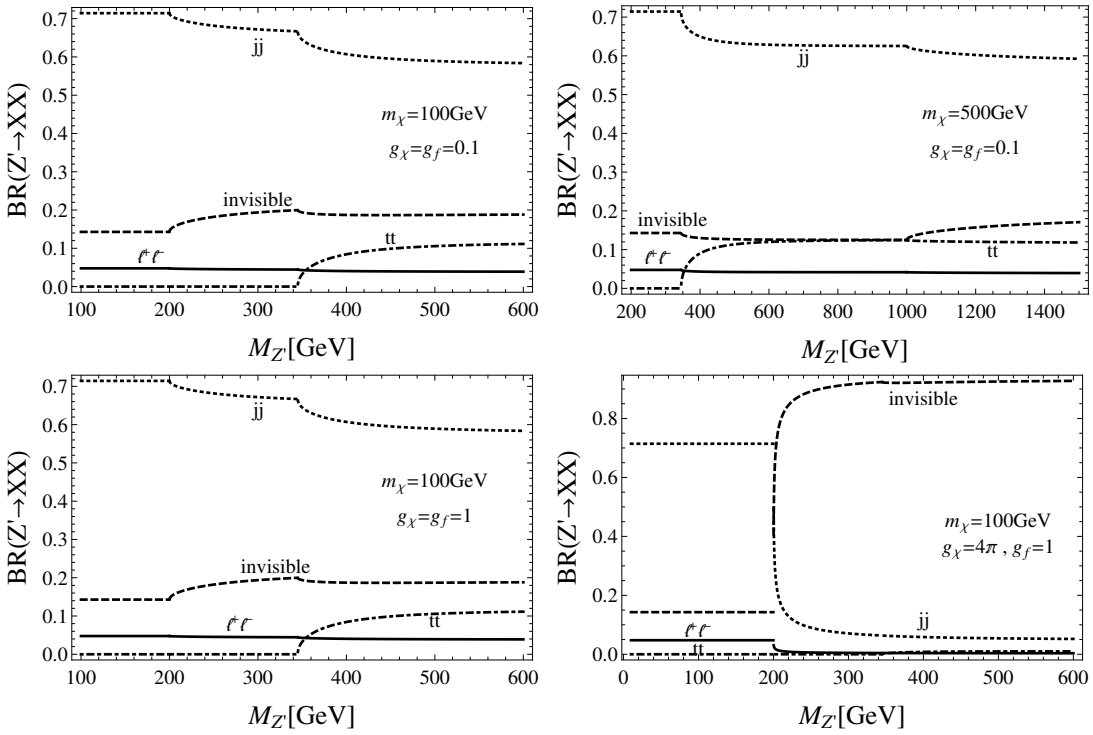


**Figure 1**. The $Z'$ branching ratios to jets, leptons (electrons, muons or taus), top quarks and invisible (DM and neutrinos), as a function of its mass $M_{Z'}$. We present four scenarios: at the left column we fix $m_\chi = 100\,\text{GeV}$, in the upper(lower) panel the couplings are chosen as $g_\chi = g_f = 0.1(1)$; at the right upper panel we choose a heavier DM with $m_\chi = 500\,\text{GeV}$ and $g_\chi = g_f = 0.1$, and in the right lower panel we show the branching ratios for an 100 GeV DM, $g_f = 1$ and $g_\chi = 4\pi$ at the boundary of the perturbative regime.

possible that a monojet search becomes as competitive as the dileptons concerning the exclusion constraints from collider data.

In the $g_f$ *versus* $M_{Z'}$ plane, the branching ratio to leptons (muons or electrons) and to invisible (DM plus neutrinos) are shown in the figure 2. In the upper, middle, and lower rows we display the branching ratios for $M_\chi = 10$, 50, and 500 GeV, respectively. In the left(right) column we fixed $g_\chi = 0.1(4\pi)$. The panels are split into two sub-panels: at left, the branching to leptons, and at right, to invisible.

In the weak DM-$Z'$ coupling regime ($g_\chi = 0.1$) and lighter DM masses ($M_\chi \leq 50\,\text{GeV}$), the branching ratio to electrons or muons reaches 4.5% for all $g_f$ until the top channel opens. The DM decays are low for all $g_f$ as can be seen at the right subpanels. In these scenarios, the dijet channel is the dominant one. As the DM masses increases, a heavy $Z'$ decays mainly to DM as $g_f$ gets small, reaching a 90% rate for $g_f \sim 0.1$. At the limit of the perturbative regime ($g_\chi = 4\pi$), a $Z'$ decays to DM predominantly, unless $g_f \gtrsim 0.4$. The branching ratio to leptons is considerably suppressed in these scenarios, being at the 1% level for $g_f \sim 1$ as we see in the right column of figure 2.



JHEP04(2017)164

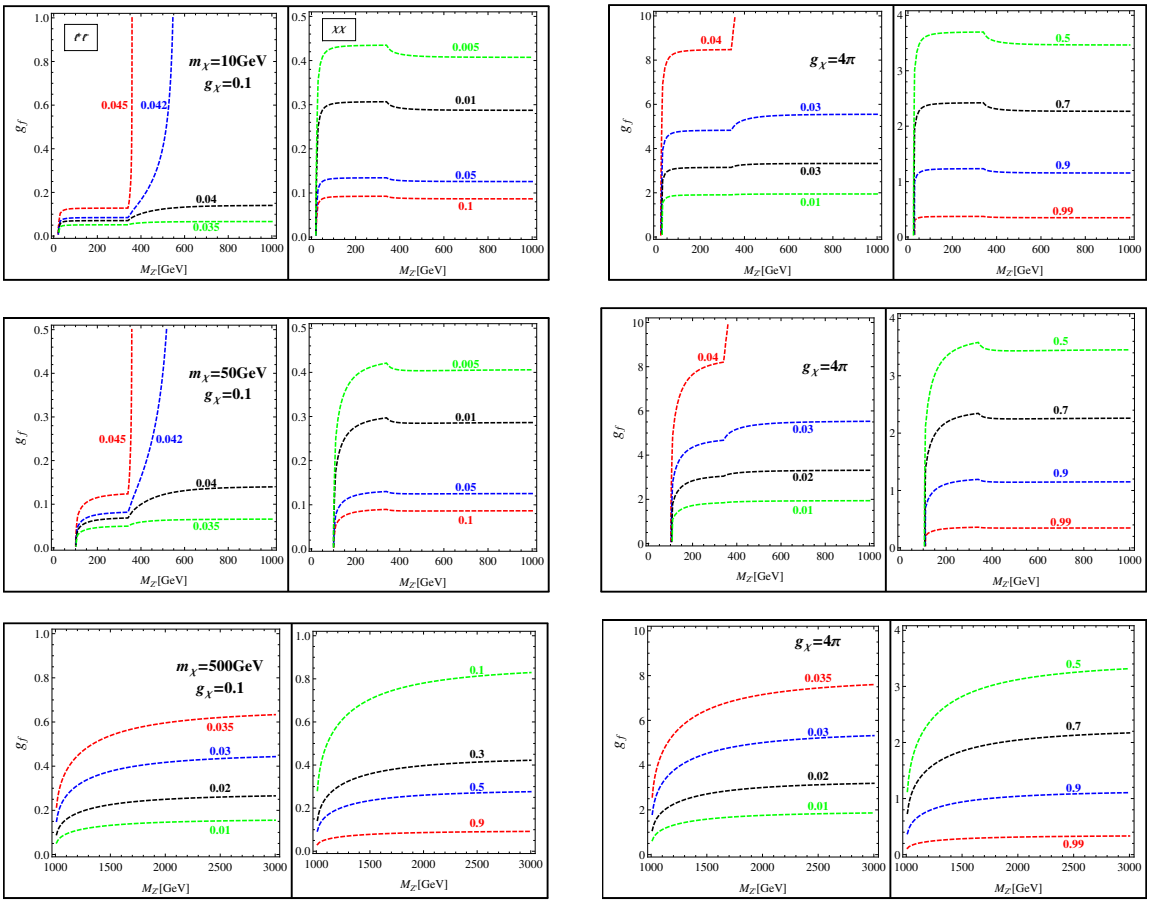


**Figure 2**. The branching ratios into leptons (electrons, muons or taus) and DM in the $M_{Z'}$ *versus* $g_f$ plane. At each pair of panels, the left one displays the branching to leptons, and the right one to dark matter. In the first, middle, and last rows we fixed $m_\chi = 10$, 50, and 500 GeV, respectively. The left column of plots have $g_\chi = 0.1$, while the at right column $g_\chi = 4\pi$. The dashed lines represent fixed branching ratios in the mass-coupling plane.

### 3.2 Searches for dimuon resonances at the 7 and 8 TeV LHC

Searches for dileptons pairs with invariant masses as low as 15 GeV have been performed by the CMS collaboration [65] at the 7 TeV run with 4.5 fb$^{-1}$. Higher invariant masses up to 4.5 TeV were probed at the 8 TeV LHC by ATLAS with $\sim$ 20 fb$^{-1}$ [66], for example, both in the dielectron as in the dimuon channel.

We use the low and high mass dimuons from the CMS and ATLAS results, respectively, in order to investigate the collider constraints on the model. Signals for muon pair production were generated with `MadGraph` [72] with one extra QCD jet, and then interfaced with `Pythia` [73] for showering and hadronization simulations. Detector effects and jet clustering were taken into account with `Delphes` [74]. Jet matching were performed in the MLM scheme [75]. The backgrounds, as the data, were taken from the experimental studies [65, 66].



JHEP04(2017)164

The dimuons pairs were selected according to the following criteria:

**Low mass region.** In the $15 < M_{\ell\ell} < 100\,\text{GeV}$ invariant mass region, CMS 7 TeV [65] adopted very loose criteria to select dimuon pairs:

$$p_T(\mu_1) > 14\ \text{GeV}\,, \qquad p_T(\mu_2) > 9\ \text{GeV}\,, \qquad |\eta_\mu| < 2.4 \tag{3.1}$$

**High mass region.** To search for high mass resonances, $M_{\ell\ell} > 100\,\text{GeV}$, with muon pairs, ATLAS 8 TeV [66] impose somewhat tighter cuts

$$p_T(\mu_1) > 25\ \text{GeV}\,, \qquad p_T(\mu_2) > 25\ \text{GeV}\,, \qquad |\eta_\mu| < 2.47 \tag{3.2}$$

Moreover, the muons are required to be isolated. We adopted the same isolation criteria of the experimental collaborations in the `Delphes` settings. Be aware the slightly stronger limits are currently available from the LHC run-II with 13 TeV using 13.3 $\text{fb}^{-1}$ of data for $m_{Z'} > 500\,\text{GeV}$ [76]. We estimate these limits to be stronger by a factor of 1.3 on the $Z'$ mass. Since our focus is on light $Z'$ gauge bosons, and our conclusions do not change even with the inclusion of more recent data, we simply keep this older data set.

### 3.3 Statistical analysis and estimated bounds

To estimate the bounds imposed on the $Z'$ masses and couplings we compared the dimuon invariant mass distributions of signal, background and data in the low and high mass regions with

$$\chi^2(\mu_s) = \min_{\{\mu_b\}} \sum_i \frac{(d_i - \mu_s s_i - \mu_b b_i)^2}{\mu_s s_i + \mu_b b_i} \tag{3.3}$$

where $d_i$, $b_i$ and $s_i$ represent the $i$-th bin count of the $M_{\ell\ell}$ distribution for data, background and signal, respectively. Our model have two free parameters: $\mu_s$ for signal and $\mu_b$ for the background normalization. The $\mu_b$ parameter is set to the best value that fits the data for a given $\mu_s$.

We employ the $\text{CL}_\text{S}$ method [77] to determine the 95% confidence limit regions on the $M_{Z'}$ *versus* $g_f$ parameter space. First we calculate the related $q$-statistic: $q(\mu_s) = \chi^2(\mu_s) - \chi^2(\hat{\mu}_s)$ if $\mu_s > \hat{\mu}_s$, and 0 otherwise, where $\hat{\mu}_s$ is the best fit for the signal strenght. After that we obtain the bounds by requiring

$$\text{CL}_\text{S} = \frac{1 - \Phi(\sqrt{q(\mu_s)})}{1 - \Phi(\sqrt{q(\mu_s)}) - \Phi(\sqrt{q_A(\mu_s)})} = 0.05 \tag{3.4}$$

The function $\Phi$ is the cumulative probability function of the standard normal distribution and $q_A(\mu_s)$ is the value of the $q$-statistic calculated assuming $d_i = \hat{\mu}_b b_i$, that is, when data are assumed to be represented by the best background model. Fixing the DM mass and its coupling $g_\chi$ to the $Z'$ boson, we seek for the solution to eq. (3.4) in the $(M_{Z'},\, g_f)$ plane as shown in figure 3.

In the upper left panel we show the $m_\chi = 10\,\text{GeV}$ case for three different $g_\chi$ values: the lower green lines for $g_\chi \leq 0.1$, the middle red ones for $g_\chi = 1$, and the upper black ones at the boundary of the perturbative regime $g_\chi = 4\pi$. The lines are discontinued at $M_{Z'} = 100\,\text{GeV}$. The constraints for the $M_{Z'} < 100\,\text{GeV}$ were derived using the low mass



JHEP04(2017)164

region data of [65], whilst those in high mass region $M_{Z'} \geq 100\,\text{GeV}$ with data from [66]. First, we observe that the excluded regions get larger as $g_\chi$ becomes smaller once the DM cannot compete for decays with leptons and jets as can be seen at the upper row of figure 3. Note that the bounds saturate for $g_\chi < 0.1$.

In the low mass region, the collider constraints are as severe as in high mass region, concerning the values of $g_f$ excluded by the 7 and 8 TeV LHC, respectively, up to $M_{Z'} \sim 50\,\text{GeV}$. In the $Z$-pole region, the constraints get softened by virtue of the huge SM $Z$ background. Also, for heavier $Z'$ bosons, the production cross sections drop fast and the top decays are turned on rendering the $\sigma(pp \to Z') \times BR(Z' \to \mu^+\mu^-)$ very small and again escaping the collider constraints.

As $\chi$ gets heavier, the constraints become increasingly insensitive to the coupling to the $Z'$, once the DM channel remains closed until $M_{Z'} \geq 2m_\chi$. This can be seen in $m_\chi = 50$, 500 and 5000 GeV panels of figure 3. For sufficiently heavy DM or with suppressed couplings to $Z'$, couplings between the vector mediator and SM fermions as low as $\sim 5 \times 10^{-3}$ are excluded at 95% CL for $M_{Z'} \sim 30$ and 200 GeV as we observe in figure 3. These particular masses are a result of the trade off among the size of $Z'$ cross section, the branching ratio to leptons, and the relative distance of the $Z$-pole mass region.

Comparing our 95% CL limits on $g_f$ with those of ref. [69] for the $Z - Z'$ mixing parameter $\epsilon$, after translating their $g_{ffZ'}$ coupling in terms of our $g_f$, we found agreement in their order of magnitude in the small mass region. The agreement is better for larger $\kappa$ which parametrizes the level of backgrounds systematics in ref. [69]. It should be noted that the mixed $Z'$ model [69] assumes vector-axial couplings between $Z'$ and the SM fermions, but it makes a little difference concerning the collider bounds.

## 4 Dark matter phenomenology

In this section we compare limits from collider searches with the constraints arising from DM phenomenology. These constraints consist in the requirement of the correct DM relic density and the compatibility with limits from both Direct (DD) and Indirect (ID) DM searches. The constraints are individually briefly illustrated below.

### 4.1 Relic density and indirect detection

The DM relic density is determined, for the range of couplings considered in our study, by the paradigm of thermal decoupling; as a consequence the experimentally favored value $\Omega h^2 \approx 0.11$ [1] corresponds to a suitable value of the DM thermally averged pair annihilation cross-section. The DM features two types of annihilation channels. The first is into SM fermions. The corresponding cross-section, originated by s-channel exchange of the $Z'$, is given by:

$$\sigma = \sum_f \frac{n_c}{12\pi\left[\left(s-m_{Z'}^2\right)^2 + m_{Z'}^2\Gamma_{Z'}^2\Gamma_{Z'}\right]}\sqrt{\frac{1-4m_f^2/s}{1-4m_\chi^2/s}} \times g_f^2\left[g_{\chi a}^2\left\{4m_\chi^2\left[m_f^2\left(7-\frac{6s}{m_{Z'}^2}+\frac{3s^2}{m_{Z'}^4}\right)-s\right]+s\left(s-4m_f^2\right)\right\}+g_{\chi v}^2(s-4m_f^2)(2m_\chi^2+s)\right], \tag{4.1}$$



JHEP04(2017)164

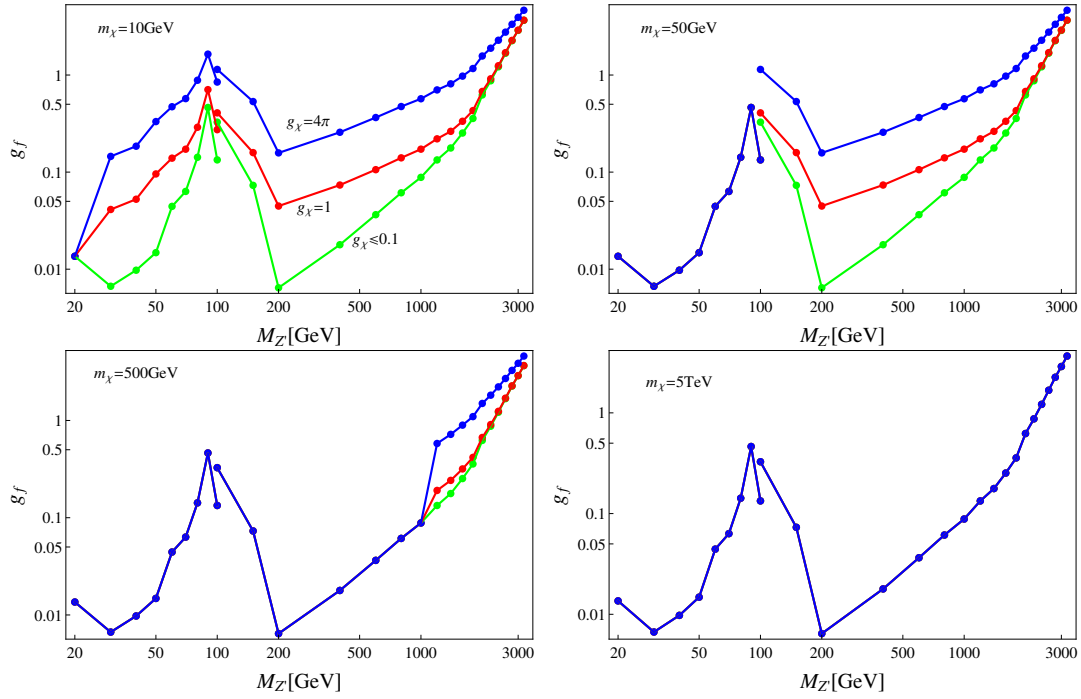


**Figure 3**. The 95% CL exclusion regions from the searches for dimuon resonances at the 7 and 8 TeV LHC. Four different DM masses and three DM-$Z'$ couplings were chosen to illustrate the collider bounds from those experiments. The constraints for the various $g_\chi$ degenerate into a single bound in the region $M_{Z'} \leq 2m_\chi$. The lines are discontinued at $M_{Z'} = 100\,\text{GeV}$, the point we chose to switch from the CMS 7 TeV data [65] to the ATLAS 8 TeV data [66].

where $n_c = 3$ (1) for annihilations to quarks (leptons), $\sqrt{s}$ is the center-of-mass energy of the collision, and $\Gamma_{Z'}$ is width of the $Z'$:

$$\Gamma(Z') = \sum_f \theta(m_{Z'} - 2m_f)\frac{n_c m_{Z'}}{24\pi}\sqrt{1-\frac{4m_f^2}{m_{Z'}^2}}\left[g_f^2\left(1-\frac{4m_f^2}{m_{Z'}^2}\right)+g_f^2\left(1+2\frac{m_f^2}{m_{Z'}^2}\right)\right]$$
$$\times\theta(m_{Z'} - 2m_\chi)\frac{m_{Z'}}{24\pi}\sqrt{1-\frac{4m_\chi^2}{m_{Z'}^2}}\left[g_{\chi a}^2\left(1-\frac{4m_\chi^2}{m_{Z'}^2}\right)+g_{\chi v}^2\left(1+2\frac{m_\chi^2}{m_{Z'}^2}\right)\right] \quad (4.2)$$

An analytic expression of the thermally averaged cross-section can be obtained through the velocity expansion [67, 78]:

$$\sigma v \approx \frac{n_c\sqrt{1-m_f^2/m_\chi^2}}{2\pi m_{Z'}^4\left(m_{Z'}^2-4m_\chi^2\right)^2}\, g_f^2\left[m_f^2 g_{\chi a}^2\left(m_{Z'}^2-4m_\chi^2\right)^2+2g_{\chi v}^2 m_{Z'}^4\left(m_\chi^2-m_f^2\right)\right] \quad (4.3)$$
$$-\frac{n_c v^2}{48\pi m_{Z'}^4 m_\chi^2\sqrt{1-m_f^2/m_\chi^2}\left(4m_\chi^2-m_{Z'}^2\right)^3}\, g_f^2\left[g_{\chi a}^2\left(m_{Z'}^2-4m_\chi^2\right)\times\right.$$



JHEP04(2017)164

$$\times\Big(m_f^4\left(-72m_{Z'}^2m_\chi^2+17m_{Z'}^4+144m_\chi^4\right)+m_f^2\left(48m_{Z'}^2m_\chi^4-22m_{Z'}^4m_\chi^2-96m_\chi^6\right)+8m_{Z'}^4m_\chi^4\Big)$$
$$-2g_{\chi v}^2m_{Z'}^4\left(m_f^2-m_\chi^2\right)\left(4m_\chi^2\left(m_{Z'}^2-17m_f^2\right)+5m_f^2m_{Z'}^2+32m_\chi^4\right)\Big].$$

In addition, if $m_\chi > m_{Z'}$, the t-channel induced $\bar{\chi}\chi \to Z'Z'$ process is kinematically allowed. The analytic expression of $\sigma(s)$ is rather contrived. We will then just report the velocity expansion given by:

$$\langle\sigma v\rangle_{Z'Z'} \approx \Bigg(\frac{\left(m_\chi^2-m_{Z'}^2\right)^{3/2}\left(g_{a\chi}^4m_{Z'}^2+2g_{a\chi}^2g_{v\chi}^2\left(4m_\chi^2-3m_{Z'}^2\right)+m_{Z'}^2g_{v\chi}^4\right)}{\pi m_\chi\left(m_{Z'}^3-2m_\chi^2m_{Z'}\right)^2}$$
$$+\frac{\sqrt{m_\chi^2-m_{Z'}^2}}{4\pi m_\chi\left(m_{Z'}^3-2m_\chi^2m_{Z'}\right)^4}\left(m_{Z'}^6g_{v\chi}^4\left(76m_\chi^4+23m_{Z'}^4-66m_\chi^2m_{Z'}^2\right)\right.$$
$$-2g_{a\chi}^2m_{Z'}^2g_{v\chi}^2\left(160m_\chi^8+21m_{Z'}^8-182m_\chi^2m_{Z'}^6+508m_\chi^4m_{Z'}^4-528m_\chi^6m_{Z'}^2\right)$$
$$\left.\times g_{a\chi}^4\left(128m_\chi^{10}+23m_{Z'}^{10}-118m_\chi^2m_{Z'}^8+172m_\chi^4m_{Z'}^6+32m_\chi^6m_{Z'}^4-192m_\chi^8m_{Z'}^2\right)\right)\Bigg). \quad (4.4)$$

These analytical approximations have been validated by numerically computing the thermally averaged cross-sections through the package Micromegas [79].

Few remarks are in order:

(i) Notice that as long as $g_{\chi v}$ is not much smaller than $g_{\chi a}$ the annihilation cross-section into SM fermions is s-wave dominated, with the dark matter annihilating nearly equally to all SM fermions, except for the color index, which makes the overall annihilation to be mostly into quarks;

(ii) The term that goes with $g_{\chi v}^2$, not helicity suppressed, gives rise to a detectable indirect detection signal at Telescopes.

(iii) The terms proportional to $g_{a\chi}$ in the first part of the eq.(4.3) is not velocity suppressed, whereas the latter is;

(iv) When the annihilation into $Z'$ pairs is turned on, even the term proportional to $g_{a\chi}$ is no longer velocity suppressed.

(v) If we had taken $g_{\chi v} = 0$, as would occur for Majorana dark matter, the $Z'$ resonance would not have been present, since the pole $(m_{Z'}^2 - 4m_\chi^2)$ in the numerator cancels out with the denominator.

Keeping that in mind, we have delimited the region that sets the right relic abundance as well as the indirect detection limits from the Fermi-LAT telescope from the observation of dwarf spheroidal galaxies [80].[3]

[3]See [81–86] for competitive limits.



JHEP04(2017)164

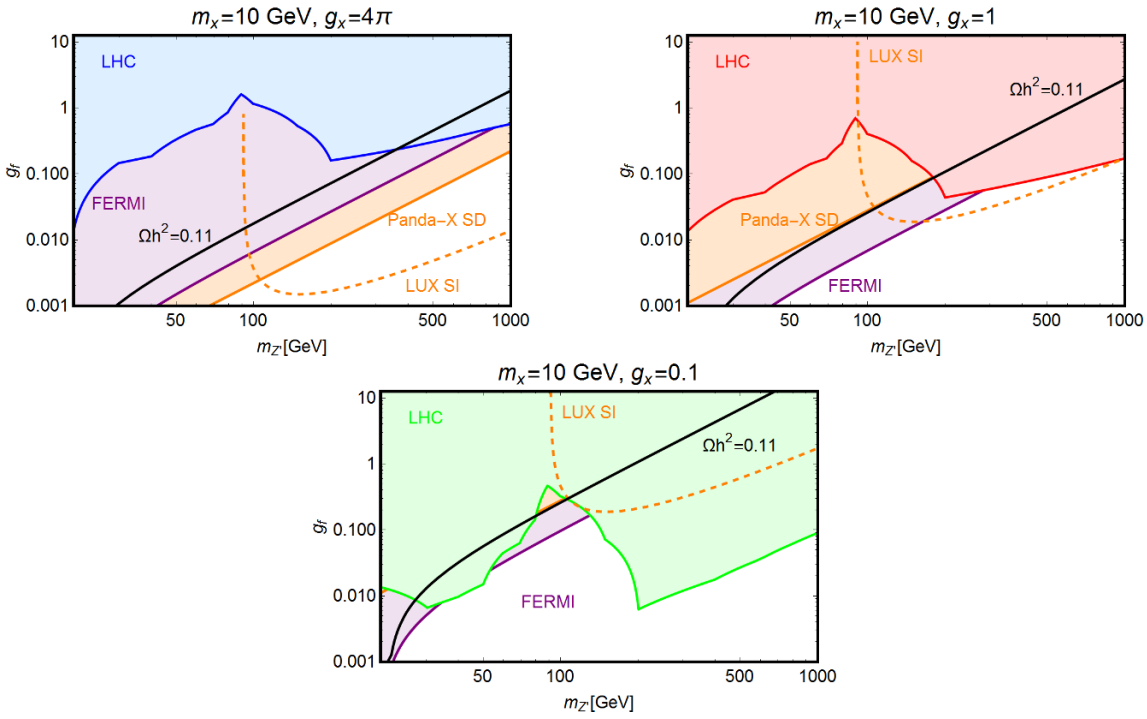


**Figure 4**. *Results for* $m_\chi = 10\,\text{GeV}$ and $g_\chi = 4\pi, 1$ and 0.1. Combined upper bounds on the model under study, in the bidimensional plane $(m_{Z'}, g_f)$ for the assignations of the DM mass $m_\chi$ and coupling $g_\chi$ reported in the different panels. The black lines delimit the correct relic density parameter space. The blue, red and green regions are excluded by LHC data. The orange region represents spin-dependent PANDA-X exclusion region, whereas the dashed curve the spin-independent LUX limit, while in purple FERMI-LAT bound.

### 4.2 Direct dark matter detection

In the case of of a $Z'$ with purely axial couplings to quarks one would expect only the spin-dependent interaction between DM and nucleons to be sizable. These are induced by the combination of the axial couplings of the $Z'$ with DM and light quarks and the corresponding cross-section is given by (we will consider only the case of scattering on neutrons since it suffers at the moment the most stringent constraints. Notice that in the case of flavor universal couplings the scattering cross sections on protons and neutrons are substantially equal.):

$$\sigma^{\text{SD (per neutron)}} \approx \frac{3\mu^2_{\chi\text{neut}}}{\pi}\frac{g^2_{\chi a}}{m^4_{Z'}}\left[g_{ua}\Delta^{\text{neut}}_u + g_{da}\left(\Delta^{\text{neut}}_d + \Delta^{\text{neut}}_s\right)\right]^2, \tag{4.5}$$

where $g_{ua}, g_{da}$ are the vector-axial couplings between the Z' and the up and down quarks respetively, which we assume to be $g_f$ according to eq. (2.2), $\mu_{\chi n}$ is the WIMP-nucleon reduced mass while $\Delta^{\text{neut}}_q$ are the quark spin fractions of the neutron. We will take these to be $\Delta^{\text{neut}}_u = -0.42$, $\Delta^{\text{neut}}_d = 0.85$, $\Delta^{\text{neut}}_s = -0.08$ [87].

The vectorial coupling between the dark matter fermion and the $Z'$, $g_{\chi v}$, is completely irrelevant for the spin-dependent scattering as one can see in eq. (4.5). Although, this



JHEP04(2017)164

coupling even if negligible in the initial Lagrangian, eq. (2.2), will be non zero, at the typical energy scales of the scattering processes since they are generated through by computing the renormalization group equations (RGE) as shown in ref. [88] so that a spin-independent cross section is actually induced with,

$$\begin{aligned}\sigma^{\text{SI (per nucleon)}} &\approx \frac{a^2\mu_{\chi n}^2}{\pi}\left[\frac{Z f_{\text{prot}} + (A-Z) f_{\text{neut}}}{A}\right]^2 \\ f_{\text{prot}} &\equiv \frac{g_{\chi \text{v}}}{m_{Z'}^2}\left(2\tilde{g}_{u\text{v}} + \tilde{g}_{d\text{v}}\right) \\ f_{\text{neut}} &\equiv \frac{g_{\chi \text{v}}}{m_{Z'}^2}\left(\tilde{g}_{u\text{v}} + 2\tilde{g}_{d\text{v}}\right)\end{aligned} \tag{4.6}$$

where $g_{uv}, g_{dv}$ are the vector couplings between the Z' and the up and down quarks respetively, which we are computed through RGE effects.

Because of the coherent scattering produced by spin-independent WIMP-nucleon interaction, the spin-independent limits are much more restrictive than the spin-dependent ones, for this reason, the spin-independent scattering even if radiatively induced may provide stronger limits in certain regions of the parameter space we we will show below. For the RGE induced $\tilde{g}_{u,d\text{v}} = \tilde{g}_{u,d\text{v}}(\mu_N), \mu_N \sim 1$ GeV couplings we have adopted, for simplicity, the analytical approximation provided in appendix B of [88], retaining only the dominant contribution, induced by top quark loops, present only above the EW scale, i.e. $m_{Z'} \gtrsim m_Z$. For $m_{Z'} < m_Z$ the spin-dependent limits from PANDA-X are more restrictive and for this reason the spin-independent ones below the Z-pole are not shown in the figures. In the figures we have considered the most recent limits from spin-dependent limits from the PANDA-X experiment [89], spin-independent from LUX [90].

Note that had we started with a Majorana dark matter particle from the beginning, $g_{v\chi}$ would always have vanished, and the RG running effect would have been irrelevant. In this case, only spin-dependent limits would be applicable, the dark matter relic density annihilation cross section would not significantly change, as well as the collider bounds agreeing with [91]. Altough, we have a sizable change as far as indirect dark matter detection is concerned since in the case of Majorana (or more in general only axial couplings of the DM with the Z') DM the s-wave component of the annihilation cross-section is helicity suppressed so at late times the annihilation cross-section of the DM is small.

That said, our findings are also applicable to Majorana Dark Matter, with mild quantitative changes, by simply ignoring the Fermi-LAT limits, as well as the spin-independent limits arising from the RG running and keeping the PANDA-X spin-dependent bounds. At the end, the model would be less constrained by data, since the spin-independent limits from LUX rule out a significant region of the parameter space.

### 4.3 Summary of results

The results of our DM analysis are summarized in figures 4–6. Here we have superimposed, for the benchmarks considered in figure 3, the collider limits from di-muon searches with the isocontours of the correct DM relic density, the limits from spin-dependent cross-section, as recently determined by the PANDA-X experiment [89], spin-independent cross-section,



JHEP04(2017)164

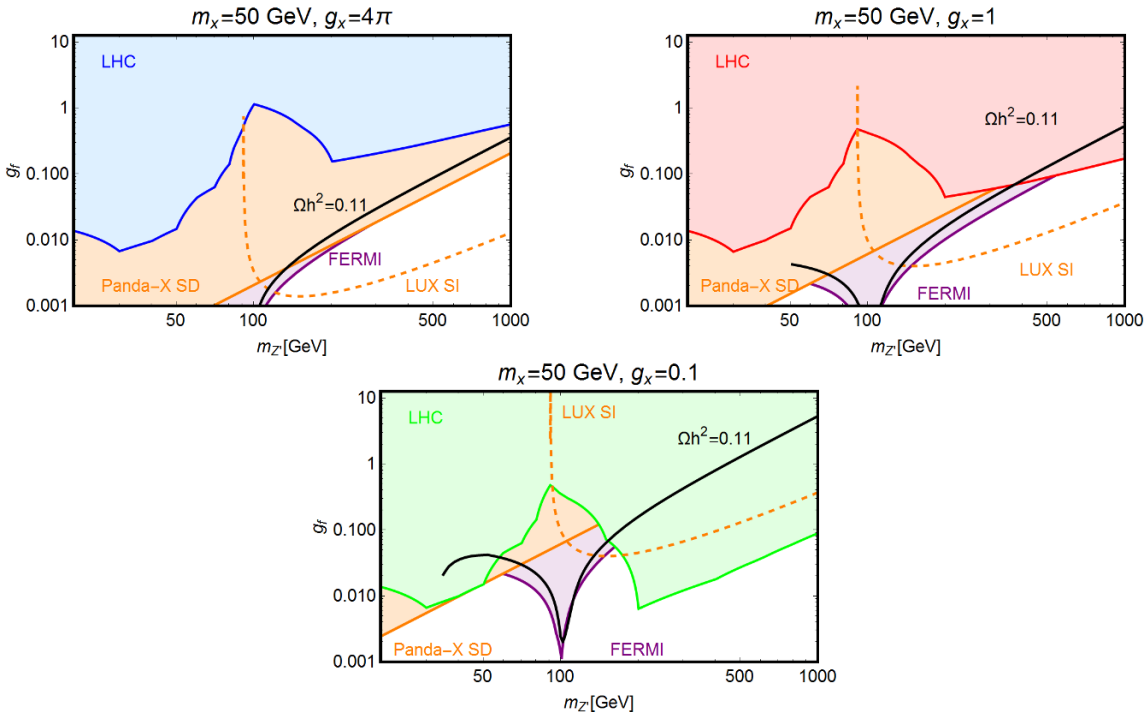


**Figure 5**. *Results for* $m_\chi = 50\,\text{GeV}$ and $g_\chi = 4\pi, 1$ and 0.1. Combined upper bounds on the model under study, in the bidimensional plane $(m_{Z'}, g_f)$ for the assignations of the DM mass $m_\chi$ and coupling $g_\chi$ reported in the different panels. The black lines delimit the correct relic density parameter space. The blue, red and green regions are excluded by LHC data. The orange region represents spin-dependent PANDA-X exclusion region, whereas the dashed curve the spin-independent LUX limit, while in purple FERMI-LAT bound.

as given by LUX [90], and the most recent limits from indirect searches of DM gamma-ray signals in DSPh [80].[4]

As already indicated, despite the radiative origin, SI interaction give stronger constraints with respect to SD ones for certain $Z'$ masses. SD limits provide nevertheless a solid complement, especially at light $Z'$ masses. Direct detection limits are competitive, or even stronger that the one from LHC for $g_\chi \gtrsim 1$ while the latter dominate for lower values of the DM couplings. Once the FERMI exclusion limit is taken into account, the light DM benchmark, $m_\chi = 10\,\text{GeV}$ is completely ruled out for $g_f \leq 10^{-3}$. Thermal DM is still in tension with ID limits for mass of 50 GeV ad exception of the pole region, $m_\chi \sim m_{Z'}/2$, where mismatch between the annihilation cross-section at freeze-out and at present times is induced by the so called thermal broadening [94, 95].

Viable thermal DM can be obtained, far from the pole region, for higher values of the mass, e.g. $m_\chi = 500\text{GeV}$, as considered in the last row of figure 6. Notice that, with the exception of the case $g_\chi = 0.1$, there are no regions with the viable DM relic density for

[4]Low energy observables, such as the muon magnetic moment, also give rise to constraints on the $Z'$ mass, but these lie around 100 GeV for couplings of order one, thus not relevant for our reasoning [92]. Moreover notice that our $Z'$ model is not ison-spin violating, otherwise a different set of bounds would be applicable [93].



JHEP04(2017)164

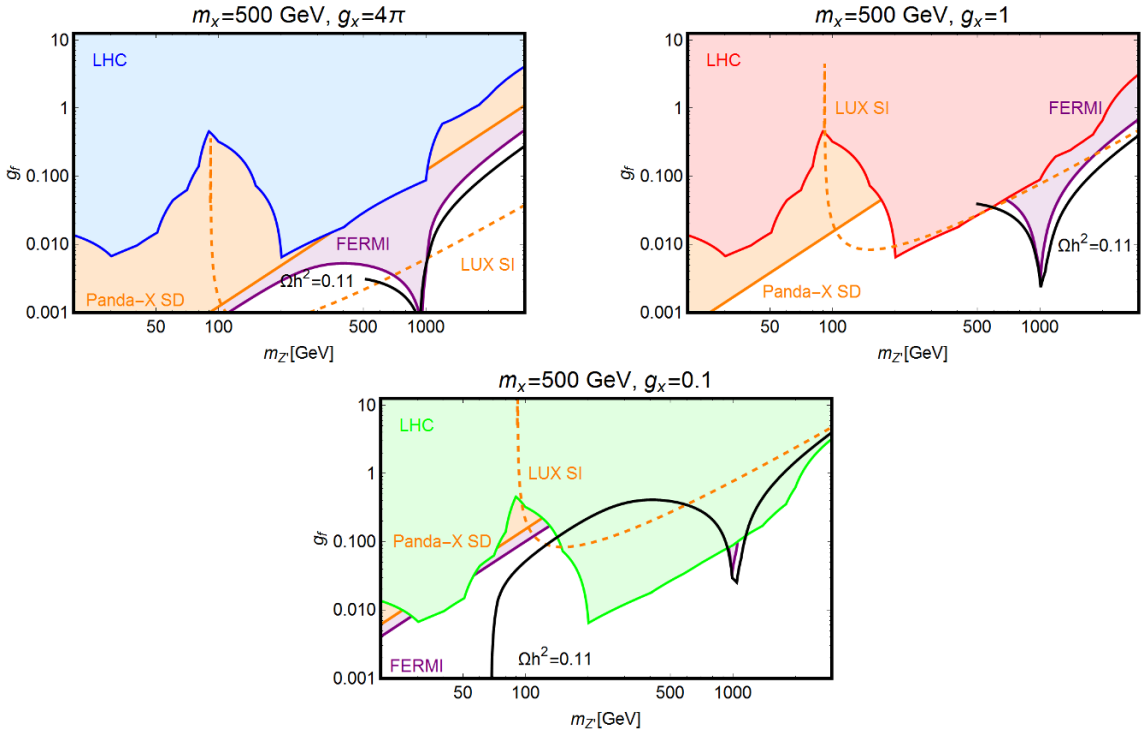


**Figure 6**. *Results for* $m_\chi = 500\,\text{GeV}$ and $g_\chi = 4\pi, 1$ and 0.1. Combined upper bounds on the model under study, in the plane $(m_{Z'}, g_f)$ for the a given DM mass $m_\chi$ and coupling $g_\chi$, as reported in the different panels. The black lines delimit the correct relic density parameter space. The blue, red and green regions are excluded by LHC data. The orange region represents spin-dependent PANDA-X exclusion region, whereas the dashed curve the spin-independent LUX limit; finally the purple region indicates the FERMI-LAT bound.

$m_\chi > m_{Z'}$. Indeed because of the $m_\chi^2/m_{Z'}^2$ enhancement and of the high values of the couplings, the DM acquires a very large annihilation cross-section into $Z'$ pair as soon as this channel becomes kinematically accessible, so that its relic density is largely suppressed with respect to the experimental expectations. For this same reason, contrary to figure 3, there are no plots relative to $m_\chi = 5\,\text{TeV}$ since, in this case, the DM relic density results always several order of magnitude below the correct value, for the couplings choices.

We stress that our results are also applicable to Majorana dark matter, because had we adopted a Majorana dark matter fermion the vectorial coupling $g_{v\chi}$ would have always been zero, and the RG running effect would have been irrelevant. In this case, only spin-dependent limits would have been applicable, with mild changes to the annihilation cross section and collider bounds. As one can see from the figures, the Majorana dark matter setup has a larger region of parameter space allowed by data, if one takes a more conservative indirect detection limit from Fermi-LAT (as we discuss in the next section). In particular, if Fermi-LAT limits are weakened, for $m_\chi = 50\,\text{GeV}$, $g_\chi = 1$ as displayed in figure 5, a much larger region of the parameter yielding the right relic abundance would be allowed by data.



JHEP04(2017)164

## 5 Galactic center excess

An excess in the GeV range has been observed in the Galactic center using data from the Fermi-LAT satellite [96–107]. There are several possible astrophysical explanations for, or caveats to, this excess. An attractive particle physics solution happens to be through annihilations of $30 - 60\,\text{GeV}$ WIMPs into quarks with an annihilation cross section of $1-3\times10^{-26}\,\text{cm}^3\text{s/s}$ normalized to a dark matter local density of $0.4\ \text{GeV/cm}^3$, i.e. slightly below the canonical value [104]. For the light $Z'$ model discussed here, the preferred annihilation final states is mostly to quarks, and at the resonance the annihilation cross section today is in the right ballpark of e.g. the results in [108].

Thus, the model under consideration here can indeed accommodate the GeV excess. However, current constraints from the observation of Dwarf Galaxies using Fermi-LAT data place stringent limits on the annihilation cross section today into quarks [109]. Without including uncertainties in the dark matter content of dwarf galaxies, the WIMP interpretation for the GeV excess is excluded at face value. However, a recent reassessment of the J-factor from the Fermi-LAT team, taking into account systematic uncertainties in the J-factors, weakens their limits by a factor of 2-3, thus showing that there might be still a bit of room left for the WIMP-annihilation hypothesis [80]. Our model thus offers a possible dark matter interpretation for the GeV excess, as long as a conservative limit from Fermi-LAT observation is considered.[5]

## 6 Note

Before submission of our paper we noted the work in [91] which partially overlaps with ours, but neither incorporated the spin-independent limits resulting from RG running and indirect detection limits, nor performed a detailed collider phenomenology.

## 7 Conclusions

Dirac fermion dark matter models in the context of heavy vector mediators are forced to live near the $Z'$ resonance due to the a combination of spin-independent and LHC bounds. One may switch off the $Z'$-fermions vectorial coupling, however, as indeed occurs in some UV-complete models, and consider light $Z'$ masses to circumvent spin-independent direct detection limits and LHC bounds on heavy resonance searches.

In this work, we have demonstrated that by including the evolution of the vector coupling between the energy scale of the mediator mass and the nuclear energy scale, this coupling, which becomes non-zero, gives rise to stringent independent limits, and that by properly deriving LHC bounds on vector mediators using the $CL_S$ method, the scenario is still rather constrained by data.

Considering a variety of data, stemming from spin-independent and spin-dependent direct detection, collider, and indirect detection, we showed that only the parameter space

[5] We decided not to go into the details of the astrophysical uncertainties surrounding the GeV excess itself which might shift the favored region downwards, to smaller annihilation cross section today [106].



JHEP04(2017)164

near the $Z'$ resonance region survives, and that one could possibly accommodate the gamma-ray excess for $m_\chi = 50\,\text{GeV}$. Moreover, we have discussed the applicability of our results to Majorana dark matter models.

## Acknowledgments

The authors warmly thank Paolo Panci for fruitful correspondence, Carlos Yaguna and Manfred Lindner for discussions. A. Alves acknowledges financial support from CNPq (process 307098/2014-1) and FAPESP (process 2013/22079-8). SP is partly supported by the U.S. Department of Energy grant number DE-SC0010107. Y. M. acknowledges partial support the ERC advanced grants Higgs@LHC and MassTeV. This research was also supported in part by the Research Executive Agency (REA) of the European Union under the Grant Agreement **PITN-GA2012-316704** ("HiggsTools") and has received funding from the European Union's Horizon 2020 research and innovation programme under the Marie Sklodowska-Curie grant agreement No 674896.



## References

[1] Planck collaboration, P.A.R. Ade et al., *Planck* 2015 *results. XIII. Cosmological parameters*, *Astron. Astrophys.* **594** (2016) A13 [arXiv:1502.01589] [INSPIRE].

[2] J.L. Feng, *Dark matter candidates from particle physics and methods of detection*, *Ann. Rev. Astron. Astrophys.* **48** (2010) 495 [arXiv:1003.0904] [INSPIRE].

[3] J. Silk et al., *Particle dark matter: observations, models and searches*, (2010).

[4] H. Baer, K.-Y. Choi, J.E. Kim and L. Roszkowski, *Dark matter production in the early universe: beyond the thermal WIMP paradigm*, *Phys. Rept.* **555** (2015) 1 [arXiv:1407.0017] [INSPIRE].

[5] L.E. Strigari, *Galactic searches for dark matter*, *Phys. Rept.* **531** (2013) 1 [arXiv:1211.7090] [INSPIRE].

[6] G. Bertone, D. Hooper and J. Silk, *Particle dark matter: evidence, candidates and constraints*, *Phys. Rept.* **405** (2005) 279 [hep-ph/0404175] [INSPIRE].

[7] E. Del Nobile, *Halo-independent comparison of direct dark matter detection data: a review*, *Adv. High Energy Phys.* **2014** (2014) 604914 [arXiv:1404.4130] [INSPIRE].

[8] T. Marrodán Undagoitia and L. Rauch, *Dark matter direct-detection experiments*, *J. Phys.* **G 43** (2016) 013001 [arXiv:1509.08767] [INSPIRE].

[9] F. Mayet et al., *A review of the discovery reach of directional dark matter detection*, *Phys. Rept.* **627** (2016) 1 [arXiv:1602.03781] [INSPIRE].

[10] F.S. Queiroz, W. Rodejohann and C.E. Yaguna, *Is the dark matter particle its own antiparticle?*, arXiv:1610.06581 [INSPIRE].



JHEP04(2017)164

[11] S. Profumo, *Astrophysical probes of dark matter*, in *Proceedings, Theoretical Advanced Study Institute in Elementary Particle Physics: Searching for New Physics at Small and Large Scales (TASI 2012)*, Boulder U.S.A., 4–29 June 2012, pg. 143 [arXiv:1301.0952] [INSPIRE].

[12] J. Conrad, *Indirect detection of WIMP dark matter: a compact review*, in *Interplay between Particle and Astroparticle physics (IPA2014)*, London U.K., 18–22 August 2014 [arXiv:1411.1925] [INSPIRE].

[13] F.S. Queiroz, *Dark matter overview: collider, direct and indirect detection searches*, arXiv:1605.08788 [INSPIRE].

[14] N. Fornengo, R.A. Lineros, M. Regis and M. Taoso, *Galactic synchrotron emission from WIMPs at radio frequencies*, *JCAP* **01** (2012) 005 [arXiv:1110.4337] [INSPIRE].

[15] Y. Mambrini, M.H.G. Tytgat, G. Zaharijas and B. Zaldivar, *Complementarity of galactic radio and collider data in constraining WIMP dark matter models*, *JCAP* **11** (2012) 038 [arXiv:1206.2352] [INSPIRE].

[16] D. Abercrombie et al., *Dark matter benchmark models for early LHC run-2 searches: report of the ATLAS/CMS dark matter forum*, arXiv:1507.00966 [INSPIRE].

[17] J. Edsjo and P. Gondolo, *Neutralino relic density including coannihilations*, *Phys. Rev.* **D 56** (1997) 1879 [hep-ph/9704361] [INSPIRE].

[18] K. Griest, *Cross-sections, relic abundance and detection rates for neutralino dark matter*, *Phys. Rev.* **D 38** (1988) 2357 [*Erratum ibid.* **D 39** (1989) 3802] [INSPIRE].

[19] S. Profumo, *TeV gamma-rays and the largest masses and annihilation cross sections of neutralino dark matter*, *Phys. Rev.* **D 72** (2005) 103521 [astro-ph/0508628] [INSPIRE].

[20] C. Garcia-Cely and J. Heeck, *Phenomenology of left-right symmetric dark matter*, *JCAP* **03** (2016) 021 [arXiv:1512.03332] [INSPIRE].

[21] C. Karwin, S. Murgia, T.M.P. Tait, T.A. Porter and P. Tanedo, *Dark matter interpretation of the Fermi-LAT observation toward the galactic center*, arXiv:1612.05687 [INSPIRE].

[22] J.K. Mizukoshi, C.A. de S. Pires, F.S. Queiroz and P.S. Rodrigues da Silva, *WIMPs in a* 3-3-1 *model with heavy sterile neutrinos*, *Phys. Rev.* **D 83** (2011) 065024 [arXiv:1010.4097] [INSPIRE].

[23] D. Cogollo, A.V. de Andrade, F.S. Queiroz and P. Rebello Teles, *Novel sources of flavor changed neutral currents in the* $331_{RHN}$ *model*, *Eur. Phys. J.* **C 72** (2012) 2029 [arXiv:1201.1268] [INSPIRE].

[24] J.D. Ruiz-Alvarez, C.A. de S. Pires, F.S. Queiroz, D. Restrepo and P.S. Rodrigues da Silva, *On the connection of gamma-rays, dark matter and Higgs searches at LHC*, *Phys. Rev.* **D 86** (2012) 075011 [arXiv:1206.5779] [INSPIRE].

[25] D. Cogollo, A.X. Gonzalez-Morales, F.S. Queiroz and P.R. Teles, *Excluding the light dark matter window of a* 331 *model using LHC and direct dark matter detection data*, *JCAP* **11** (2014) 002 [arXiv:1402.3271] [INSPIRE].

[26] R. Martínez, J. Nisperuza, F. Ochoa and J.P. Rubio, *Scalar dark matter with CERN-LEP data and* $Z'$ *search at the LHC in an* $\mathrm{U}(1)'$ *model*, *Phys. Rev.* **D 90** (2014) 095004 [arXiv:1408.5153] [INSPIRE].

JHEP04(2017)164

[27] C. Kelso, H.N. Long, R. Martinez and F.S. Queiroz, *Connection of $g-2_\mu$, electroweak, dark matter and collider constraints on* 331 *models*, *Phys. Rev.* **D 90** (2014) 113011 [arXiv:1408.6203] [INSPIRE].

[28] A. Alves, S. Profumo, F.S. Queiroz and W. Shepherd, *Effective field theory approach to the galactic center gamma-ray excess*, *Phys. Rev.* **D 90** (2014) 115003 [arXiv:1403.5027] [INSPIRE].

[29] B. Allanach, F.S. Queiroz, A. Strumia and S. Sun, *$Z'$ models for the LHCb and $g-2$ muon anomalies*, *Phys. Rev.* **D 93** (2016) 055045 [arXiv:1511.07447] [INSPIRE].

[30] P.V. Dong, N.T.K. Ngan and D.V. Soa, *Simple* 3-3-1 *model and implication for dark matter*, *Phys. Rev.* **D 90** (2014) 075019 [arXiv:1407.3839] [INSPIRE].

[31] P.V. Dong, C.S. Kim, D.V. Soa and N.T. Thuy, *Investigation of dark matter in minimal* 3-3-1 *models*, *Phys. Rev.* **D 91** (2015) 115019 [arXiv:1501.04385] [INSPIRE].

[32] A. Alves, G. Arcadi, P.V. Dong, L. Duarte, F.S. Queiroz and J.W.F. Valle, *R-parity as a residual gauge symmetry: probing a theory of cosmological dark matter*, arXiv:1612.04383 [INSPIRE].

[33] P. Gondolo, P. Ko and Y. Omura, *Light dark matter in leptophobic $Z'$ models*, *Phys. Rev.* **D 85** (2012) 035022 [arXiv:1106.0885] [INSPIRE].

[34] H. An, R. Huo and L.-T. Wang, *Searching for low mass dark portal at the LHC*, *Phys. Dark Univ.* **2** (2013) 50 [arXiv:1212.2221] [INSPIRE].

[35] S. Profumo and F.S. Queiroz, *Constraining the $Z'$ mass in* 331 *models using direct dark matter detection*, *Eur. Phys. J.* **C 74** (2014) 2960 [arXiv:1307.7802] [INSPIRE].

[36] A. Alves, S. Profumo and F.S. Queiroz, *The dark $Z'$ portal: direct, indirect and collider searches*, *JHEP* **04** (2014) 063 [arXiv:1312.5281] [INSPIRE].

[37] G. Arcadi, Y. Mambrini, M.H.G. Tytgat and B. Zaldivar, *Invisible $Z'$ and dark matter: LHC vs LUX constraints*, *JHEP* **03** (2014) 134 [arXiv:1401.0221] [INSPIRE].

[38] A. De Simone, G.F. Giudice and A. Strumia, *Benchmarks for dark matter searches at the LHC*, *JHEP* **06** (2014) 081 [arXiv:1402.6287] [INSPIRE].

[39] J.M. Cline, G. Dupuis, Z. Liu and W. Xue, *The windows for kinetically mixed $Z'$-mediated dark matter and the galactic center gamma ray excess*, *JHEP* **08** (2014) 131 [arXiv:1405.7691] [INSPIRE].

[40] N. Chen, Y. Zhang, Q. Wang, G. Cacciapaglia, A. Deandrea and L. Panizzi, *Higgsphobic and fermiophobic $Z'$ as a single dark matter candidate*, *JHEP* **05** (2014) 088 [arXiv:1403.2918] [INSPIRE].

[41] W.-Z. Feng, G. Shiu, P. Soler and F. Ye, *Probing hidden sectors with Stückelberg* U(1) *gauge fields*, *Phys. Rev. Lett.* **113** (2014) 061802 [arXiv:1401.5880] [INSPIRE].

[42] O. Lebedev and Y. Mambrini, *Axial dark matter: the case for an invisible $Z'$*, *Phys. Lett.* **B 734** (2014) 350 [arXiv:1403.4837] [INSPIRE].

[43] P.V. Dong, D.T. Huong, F.S. Queiroz and N.T. Thuy, *Phenomenology of the* 3-3-1-1 *model*, *Phys. Rev.* **D 90** (2014) 075021 [arXiv:1405.2591] [INSPIRE].

[44] F. Kahlhoefer, K. Schmidt-Hoberg, T. Schwetz and S. Vogl, *Implications of unitarity and gauge invariance for simplified dark matter models*, *JHEP* **02** (2016) 016 [arXiv:1510.02110] [INSPIRE].



JHEP04(2017)164

[45] C. Marcos, M. Peiro and S. Robles, *On the importance of direct detection combined limits for spin independent and spin dependent dark matter interactions*, *JCAP* **03** (2016) 019 [arXiv:1507.08625] [INSPIRE].

[46] M. Chala, F. Kahlhoefer, M. McCullough, G. Nardini and K. Schmidt-Hoberg, *Constraining dark sectors with monojets and dijets*, *JHEP* **07** (2015) 089 [arXiv:1503.05916] [INSPIRE].

[47] N. Chen, J. Wang and X.-P. Wang, *The leptophilic dark matter with $Z'$ interaction: from indirect searches to future $e^+e^-$ collider searches*, arXiv:1501.04486 [INSPIRE].

[48] O. Ducu, L. Heurtier and J. Maurer, *LHC signatures of a $Z'$ mediator between dark matter and the* SU(3) *sector*, *JHEP* **03** (2016) 006 [arXiv:1509.05615] [INSPIRE].

[49] V.M. Lozano, M. Peiró and P. Soler, *Isospin violating dark matter in Stückelberg portal scenarios*, *JHEP* **04** (2015) 175 [arXiv:1503.01780] [INSPIRE].

[50] C.-W. Chiang, T. Nomura and K. Yagyu, *Leptophobic $Z'$ in models with multiple Higgs doublet fields*, *JHEP* **05** (2015) 127 [arXiv:1502.00855] [INSPIRE].

[51] N. Okada and S. Okada, *$Z'$-portal right-handed neutrino dark matter in the minimal* $\mathrm{U}(1)_X$ *extended Standard Model*, *Phys. Rev.* **D 95** (2017) 035025 [arXiv:1611.02672] [INSPIRE].

[52] A. Celis, W.-Z. Feng and M. Vollmann, *Dirac dark matter and $b \to s\ell^+\ell^-$ with* U(1) *gauge symmetry*, *Phys. Rev.* **D 95** (2017) 035018 [arXiv:1608.03894] [INSPIRE].

[53] M. Klasen, F. Lyonnet and F.S. Queiroz, *NLO+NLL collider bounds, Dirac fermion and scalar dark matter in the $B$-$L$ model*, arXiv:1607.06468 [INSPIRE].

[54] N.F. Bell, Y. Cai and R.K. Leane, *Impact of mass generation for spin-1 mediator simplified models*, *JCAP* **01** (2017) 039 [arXiv:1610.03063] [INSPIRE].

[55] P. Ko and T. Nomura, *Phenomenology of dark matter in chiral* $\mathrm{U}(1)_X$ *dark sector*, *Phys. Rev.* **D 94** (2016) 115015 [arXiv:1607.06218] [INSPIRE].

[56] M. Duerr, F. Kahlhoefer, K. Schmidt-Hoberg, T. Schwetz and S. Vogl, *How to save the WIMP: global analysis of a dark matter model with two s-channel mediators*, *JHEP* **09** (2016) 042 [arXiv:1606.07609] [INSPIRE].

[57] M. Fairbairn, J. Heal, F. Kahlhoefer and P. Tunney, *Constraints on $Z'$ models from LHC dijet searches and implications for dark matter*, *JHEP* **09** (2016) 018 [arXiv:1605.07940] [INSPIRE].

[58] T. Jacques, A. Katz, E. Morgante, D. Racco, M. Rameez and A. Riotto, *Complementarity of DM searches in a consistent simplified model: the case of $Z'$*, *JHEP* **10** (2016) 071 [arXiv:1605.06513] [INSPIRE].

[59] C. Englert, M. McCullough and M. Spannowsky, *s-channel dark matter simplified models and unitarity*, *Phys. Dark Univ.* **14** (2016) 48 [arXiv:1604.07975] [INSPIRE].

[60] F.S. Sage, J.N.E. Ho, T.G. Steele and R. Dick, *Remarks on top-philic $Z'$ boson interactions with nucleons*, arXiv:1611.03367 [INSPIRE].

[61] W. Altmannshofer, S. Gori, S. Profumo and F.S. Queiroz, *Explaining dark matter and B decay anomalies with an $L_\mu$-$L_\tau$ model*, *JHEP* **12** (2016) 106 [arXiv:1609.04026] [INSPIRE].

[62] N. Okada and S. Okada, *$Z'_{BL}$ portal dark matter and LHC run-2 results*, *Phys. Rev.* **D 93** (2016) 075003 [arXiv:1601.07526] [INSPIRE].

[63] Y. Bai, J. Bourbeau and T. Lin, *Dark matter searches with a mono-$Z'$ jet*, *JHEP* **06** (2015) 205 [arXiv:1504.01395] [INSPIRE].

JHEP04(2017)164

[64] A. Ismail, W.-Y. Keung, K.-H. Tsao and J. Unwin, *Axial vector $Z'$ and anomaly cancellation*, *Nucl. Phys.* **B 918** (2017) 220 [arXiv:1609.02188] [INSPIRE].

[65] CMS collaboration, *Measurement of the differential and double-differential Drell-Yan cross sections in proton-proton collisions at $\sqrt{s} = 7$ TeV*, *JHEP* **12** (2013) 030 [arXiv:1310.7291] [INSPIRE].

[66] ATLAS collaboration, *Search for high-mass dilepton resonances in pp collisions at $\sqrt{s} = 8$ TeV with the ATLAS detector*, *Phys. Rev.* **D 90** (2014) 052005 [arXiv:1405.4123] [INSPIRE].

[67] A. Alves, A. Berlin, S. Profumo and F.S. Queiroz, *Dark matter complementarity and the $Z'$ portal*, *Phys. Rev.* **D 92** (2015) 083004 [arXiv:1501.03490] [INSPIRE].

[68] A. Alves, A. Berlin, S. Profumo and F.S. Queiroz, *Dirac-fermionic dark matter in $\mathrm{U}(1)_X$ models*, *JHEP* **10** (2015) 076 [arXiv:1506.06767] [INSPIRE].

[69] I. Hoenig, G. Samach and D. Tucker-Smith, *Searching for dilepton resonances below the Z mass at the LHC*, *Phys. Rev.* **D 90** (2014) 075016 [arXiv:1408.1075] [INSPIRE].

[70] J. Alwall et al., *The automated computation of tree-level and next-to-leading order differential cross sections and their matching to parton shower simulations*, *JHEP* **07** (2014) 079 [arXiv:1405.0301] [INSPIRE].

[71] A. Alloul, J. D'Hondt, K. De Causmaecker, B. Fuks and M. Rausch de Traubenberg, *Automated mass spectrum generation for new physics*, *Eur. Phys. J.* **C 73** (2013) 2325 [arXiv:1301.5932] [INSPIRE].

[72] J. Alwall, M. Herquet, F. Maltoni, O. Mattelaer and T. Stelzer, *MadGraph 5: going beyond*, *JHEP* **06** (2011) 128 [arXiv:1106.0522] [INSPIRE].

[73] T. Sjöstrand, S. Mrenna and P.Z. Skands, *PYTHIA 6.4 physics and manual*, *JHEP* **05** (2006) 026 [hep-ph/0603175] [INSPIRE].

[74] DELPHES 3 collaboration, J. de Favereau et al., *DELPHES 3, a modular framework for fast simulation of a generic collider experiment*, *JHEP* **02** (2014) 057 [arXiv:1307.6346] [INSPIRE].

[75] M.L. Mangano, M. Moretti, F. Piccinini and M. Treccani, *Matching matrix elements and shower evolution for top-quark production in hadronic collisions*, *JHEP* **01** (2007) 013 [hep-ph/0611129] [INSPIRE].

[76] ATLAS collaboration, *Search for new high-mass resonances in the dilepton final state using proton-proton collisions at $\sqrt{s} = 13$ TeV with the ATLAS detector*, ATLAS-CONF-2016-045, CERN, Geneva Switzerland, (2016).

[77] G. Cowan, K. Cranmer, E. Gross and O. Vitells, *Asymptotic formulae for likelihood-based tests of new physics*, *Eur. Phys. J.* **C 71** (2011) 1554 [*Erratum ibid.* **C 73** (2013) 2501] [arXiv:1007.1727] [INSPIRE].

[78] G. Arcadi, Y. Mambrini and F. Richard, *Z-portal dark matter*, *JCAP* **03** (2015) 018 [arXiv:1411.2985] [INSPIRE].

[79] G. Bélanger, F. Boudjema, A. Pukhov and A. Semenov, *MicrOMEGAs4.1: two dark matter candidates*, *Comput. Phys. Commun.* **192** (2015) 322 [arXiv:1407.6129] [INSPIRE].



JHEP04(2017)164

[80] DES and Fermi-LAT collaborations, A. Albert et al., *Searching for dark matter annihilation in recently discovered milky way satellites with Fermi-LAT*, *Astrophys. J.* **834** (2017) 110 [arXiv:1611.03184] [INSPIRE].

[81] D. Hooper, C. Kelso and F.S. Queiroz, *Stringent and robust constraints on the dark matter annihilation cross section from the region of the galactic center*, *Astropart. Phys.* **46** (2013) 55 [arXiv:1209.3015] [INSPIRE].

[82] T. Bringmann and C. Weniger, *Gamma ray signals from dark matter: concepts, status and prospects*, *Phys. Dark Univ.* **1** (2012) 194 [arXiv:1208.5481] [INSPIRE].

[83] L. Bergstrom, T. Bringmann, I. Cholis, D. Hooper and C. Weniger, *New limits on dark matter annihilation from AMS cosmic ray positron data*, *Phys. Rev. Lett.* **111** (2013) 171101 [arXiv:1306.3983] [INSPIRE].

[84] A.X. Gonzalez-Morales, S. Profumo and F.S. Queiroz, *Effect of black holes in local dwarf spheroidal galaxies on gamma-ray constraints on dark matter annihilation*, *Phys. Rev.* **D 90** (2014) 103508 [arXiv:1406.2424] [INSPIRE].

[85] S. Profumo, F.S. Queiroz and C.E. Yaguna, *Extending Fermi-LAT and H.E.S.S. limits on gamma-ray lines from dark matter annihilation*, *Mon. Not. Roy. Astron. Soc.* **461** (2016) 3976 [arXiv:1602.08501] [INSPIRE].

[86] R. Caputo et al., *Search for gamma-ray emission from dark matter annihilation in the small Magellanic cloud with the Fermi Large Area Telescope*, *Phys. Rev.* **D 93** (2016) 062004 [arXiv:1603.00965] [INSPIRE].

[87] H.-Y. Cheng and C.-W. Chiang, *Revisiting scalar and pseudoscalar couplings with nucleons*, *JHEP* **07** (2012) 009 [arXiv:1202.1292] [INSPIRE].

[88] F. D'Eramo, B.J. Kavanagh and P. Panci, *You can hide but you have to run: direct detection with vector mediators*, *JHEP* **08** (2016) 111 [arXiv:1605.04917] [INSPIRE].

[89] PandaX-II collaboration, C. Fu et al., *Spin-dependent weakly-interacting-massive-particle-nucleon cross section limits from first data of PandaX-II experiment*, *Phys. Rev. Lett.* **118** (2017) 071301 [arXiv:1611.06553] [INSPIRE].

[90] LUX collaboration, D.S. Akerib et al., *Results from a search for dark matter in the complete LUX exposure*, *Phys. Rev. Lett.* **118** (2017) 021303 [arXiv:1608.07648] [INSPIRE].

[91] M. Escudero, D. Hooper and S.J. Witte, *Updated collider and direct detection constraints on dark matter models for the galactic center gamma-ray excess*, *JCAP* **02** (2017) 038 [arXiv:1612.06462] [INSPIRE].

[92] M. Lindner, M. Platscher and F.S. Queiroz, *A call for new physics: the muon anomalous magnetic moment and lepton flavor violation*, arXiv:1610.06587 [INSPIRE].

[93] C.E. Yaguna, *Isospin-violating dark matter in the light of recent data*, *Phys. Rev.* **D 95** (2017) 055015 [arXiv:1610.08683] [INSPIRE].

[94] P. Gondolo and G. Gelmini, *Cosmic abundances of stable particles: improved analysis*, *Nucl. Phys.* **B 360** (1991) 145 [INSPIRE].

[95] K. Griest and D. Seckel, *Three exceptions in the calculation of relic abundances*, *Phys. Rev.* **D 43** (1991) 3191 [INSPIRE].

[96] L. Goodenough and D. Hooper, *Possible evidence for dark matter annihilation in the inner milky way from the Fermi gamma ray space telescope*, arXiv:0910.2998 [INSPIRE].

JHEP04(2017)164

[97] D. Hooper and L. Goodenough, *Dark matter annihilation in the galactic center as seen by the Fermi gamma ray space telescope*, *Phys. Lett.* **B 697** (2011) 412 [arXiv:1010.2752] [INSPIRE].

[98] A. Boyarsky, D. Malyshev and O. Ruchayskiy, *A comment on the emission from the galactic center as seen by the Fermi telescope*, *Phys. Lett.* **B 705** (2011) 165 [arXiv:1012.5839] [INSPIRE].

[99] D. Hooper and T. Linden, *On the origin of the gamma rays from the galactic center*, *Phys. Rev.* **D 84** (2011) 123005 [arXiv:1110.0006] [INSPIRE].

[100] K.N. Abazajian and M. Kaplinghat, *Detection of a gamma-ray source in the galactic center consistent with extended emission from dark matter annihilation and concentrated astrophysical emission*, *Phys. Rev.* **D 86** (2012) 083511 [*Erratum ibid.* **D 87** (2013) 129902] [arXiv:1207.6047] [INSPIRE].

[101] D. Hooper and T.R. Slatyer, *Two emission mechanisms in the Fermi bubbles: a possible signal of annihilating dark matter*, *Phys. Dark Univ.* **2** (2013) 118 [arXiv:1302.6589] [INSPIRE].

[102] C. Gordon and O. Macias, *Dark matter and pulsar model constraints from galactic center Fermi-LAT gamma ray observations*, *Phys. Rev.* **D 88** (2013) 083521 [*Erratum ibid.* **D 89** (2014) 049901] [arXiv:1306.5725] [INSPIRE].

[103] W.-C. Huang, A. Urbano and W. Xue, *Fermi bubbles under dark matter scrutiny. Part I: astrophysical analysis*, arXiv:1307.6862 [INSPIRE].

[104] T. Daylan et al., *The characterization of the gamma-ray signal from the central milky way: a case for annihilating dark matter*, *Phys. Dark Univ.* **12** (2016) 1 [arXiv:1402.6703] [INSPIRE].

[105] K.N. Abazajian, N. Canac, S. Horiuchi and M. Kaplinghat, *Astrophysical and dark matter interpretations of extended gamma-ray emission from the galactic center*, *Phys. Rev.* **D 90** (2014) 023526 [arXiv:1402.4090] [INSPIRE].

[106] F. Calore, I. Cholis and C. Weniger, *Background model systematics for the Fermi GeV excess*, *JCAP* **03** (2015) 038 [arXiv:1409.0042] [INSPIRE].

[107] Fermi-LAT collaboration, M. Ajello et al., *Fermi-LAT observations of high-energy $\gamma$-ray emission toward the galactic center*, *Astrophys. J.* **819** (2016) 44 [arXiv:1511.02938] [INSPIRE].

[108] D. Hooper, *$Z'$ mediated dark matter models for the galactic center gamma-ray excess*, *Phys. Rev.* **D 91** (2015) 035025 [arXiv:1411.4079] [INSPIRE].

[109] Fermi-LAT collaboration, M. Ackermann et al., *Searching for dark matter annihilation from milky way dwarf spheroidal galaxies with six years of Fermi Large Area Telescope data*, *Phys. Rev. Lett.* **115** (2015) 231301 [arXiv:1503.02641] [INSPIRE].

JHEP04(2017)164